Quantum cutting mechanism in Tb3+-Yb3+ co-doped oxyfluoride glass

Qianqian Duan, Feng Qin, Dan Wang, Wei Xu, Jianmin Cheng et al.

Citation: J. Appl. Phys. **110**, 113503 (2011); doi: 10.1063/1.3662916
View online: http://dx.doi.org/10.1063/1.3662916
View Table of Contents: http://jap.aip.org/resource/1/JAPIAU/v110/i11
Published by the American Institute of Physics.

Quantum cutting mechanism in Tb^{3+}-Yb^{3+} co-doped oxyfluoride glass

Qianqian Duan,[1] Feng Qin,[1] Dan Wang,[1] Wei Xu,[1] Jianmin Cheng,[1] Zhiguo Zhang,[1,2,a)] and Wenwu Cao[1,2,3,b)]
[1]*Condensed Matter Science and Technology Institute, Harbin Institute of Technology, Harbin, 150001, China*
[2]*Laboratory of Sono- and Photo-Theranostic Technologies, Harbin Institute of Technology, Harbin, 150001, China*
[3]*Materials Research Institute, The Pennsylvania State University, University Park, Pennsylvania 16802, USA*

(Received 25 July 2011; accepted 16 October 2011; published online 1 December 2011)

Rate equations were created to describe cooperative quantum cutting phenomena, which incorporated the interactions between donor Tb^{3+} and acceptor Yb^{3+} ions. Two judgment criteria were developed for the excitation power dependence and time-resolved luminescence spectra of donor and acceptor ions, which can be used to verify the proposed mechanism. Under the excitation of a 473 nm continuous wave laser, the emission intensities of Tb^{3+} and Yb^{3+} increased linearly with the excitation power. The decay curve of Yb^{3+} indicated two distinct contributions: the fast decay time of its own lifetime, and the slow decay time representing the lifetime of the $^5D_4$ energy level of Tb^{3+}. The experimental results meet the two judgment criteria, which confirmed the proposed cooperative quantum cutting mechanism in Tb^{3+}-Yb^{3+} co-doped oxyfluoride glass. © *2011 American Institute of Physics*. [doi:10.1063/1.3662916]

I. INTRODUCTION

Quantum cutting can convert one ultraviolet/visible photon into two near infrared photons, which could be absorbed by Si solar cells to reduce thermal losses and obtain doubled current in the high energy region of the solar spectrum.[1–5] Therefore, near infrared quantum cutting is a promising option to enhance the efficiency of Si solar cells. Near infrared quantum cutting can be realized by using coupled rare earth ions due to their unique energy level structures and high quantum efficiency.[5–7] Because Yb^{3+} has only one 4f excited state and its emission band is around 1000 nm (10000 cm^{-1}), which is the most sensitive spectral region of c-Si solar cells,[2] searching for proper rare earth ions that can use the property of Yb^{3+}, has been one of the intriguing research topics in the quantum cutting field.[8]

Quantum cutting using Re^{3+}-Yb^{3+} to enhance high energy absorbing efficiency for solar cells was first reported using $Yb_xY_{1-x}PO_4$: Tb^{3+} powder samples.[9] Near infrared quantum cutting based on Tb^{3+}-Yb^{3+} pairs has also been reported in several other host materials.[10–12] In addition, other rare earth ion coupled pairs, including (Pr^{3+}, Yb^{3+}),[10,13,14] (Tm^{3+}, Yb^{3+}),[10,15] and so on, were also investigated. For the Tb^{3+}-Yb^{3+} coupled pair, the quantum cutting energy transfer was studied both experimentally and theoretically.[9] The luminescence decay curves of the donor ion (Tb^{3+}) were measured and analyzed by the Monte Carlo simulation based on different energy transfer mechanisms. It was found that the experimental results agreed better with the cooperative energy transfer model than with other models, which indicated that the cooperative energy transfer was the dominant mechanism. The cooperative quantum cutting mechanism is illustrated in Fig. 1.[10–12] One Tb^{3+} ion absorbed one blue photon with the transition from $^7F_6$ to $^5D_4$ energy level and then transferred the energy to two Yb^{3+} ions simultaneously producing two near-infrared photon emissions.

Up to now, analyses on the energy transfer mechanism mostly used the decay curves of donor ions, which did not take into account ionic interaction contributions. There is little report in the literature on decay curves of the acceptor ion, which is very important to reflect the interactions between the coupled pair ions.

Spectroscopic data, decay curves of donor ions and acceptor ions, and the excitation power dependence of luminescence intensities are essential information for understanding the excitation mechanism in luminescence.[16] It was found that there is a controversy in the excitation power dependence of Yb^{3+} luminescence intensity.[4] It is expected that the down conversion emission intensities should increase linearly with the excitation intensity,[2,3,17,18] but some papers reported a second-order process for the cooperative quantum cutting, in which the slope of the excitation power dependence curve is about 0.5 instead of 1.[19–22]

In general, all spectroscopic data could be represented in the rate equations. Rate equations include information of both donor and acceptor ions and can be used to perform multi-analysis on the energy transfer mechanism through pair ion interactions. Strek *et al*. created rate equations in a simplified three-level system to describe the down conversion process in Tb^{3+}-doped $KYb(WO_4)_2$ crystals.[19] However, to date, there has been little reported on using rate equations to study the quantum cutting mechanism.

In this paper, the quantum cutting energy transfer mechanism in Tb^{3+}-Yb^{3+} co-doped oxyfluoride glass was investigated using rate equations. On the basis of the rate equations for cooperative quantum cutting, two judgment criteria were developed. An experimental system was designed and built to measure the time-resolved spectra under the excitation of

a)Author to whom correspondence should be addressed. Electronic mail: zhangzhiguo@hit.edu.cn.
b)Electronic address: dzk@psu.edu.

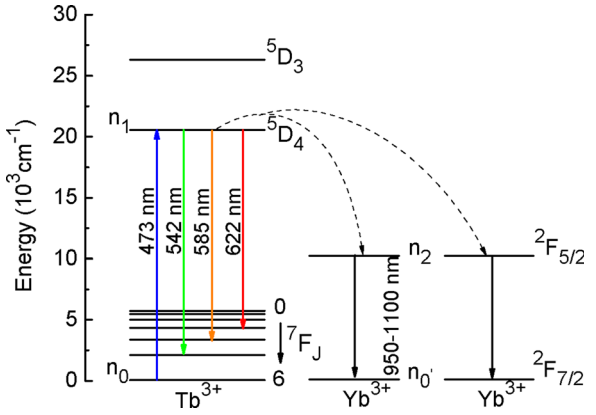

FIG. 1. (Color online) Schematic energy level diagram in Tb^{3+}-Yb^{3+} co-doped glass showing cooperative energy transfer mechanism of the near infrared quantum cutting under 473 nm laser excitation.

a 473 nm continuous wave laser. The emission spectra, time-resolved luminescence spectra of donor and acceptor ions, and excitation power dependence were carefully measured by our experimental setup. The experimental results showed good agreement with the judgment criteria of the theoretical rate equations, which justified our theoretical approach.

II. EXPERIMENTAL

A. Material synthesis

The oxyfluoride glass with compositions of $50SiO_2$-$20Al_2O_3$-$27CaF_2$-$1Tb^{3+}$-xYb^{3+} ($x = 0, 5$) were prepared by the traditional high-temperature solid-state reaction method. High purity SiO_2, Al_2O_3, CaF_2, Tb_4O_7, and Yb_2O_3 powders were mixed and ground for 1 h, then the mixture was melted in a covered corundum crucible at 1360 °C for 90 min. Subsequently, the melt mixture were poured onto a room temperature brass plate and cooled naturally in air. The obtained glasses were annealed at 500 °C for 3 h to release the internal stresses. Finally, the glass was cut and polished into samples 2 mm thick.

B. Luminescence spectroscopy

A 473 nm continuous wave laser with a maximum power of 450 mW was used as the excitation source. The emission spectra were recorded by a lens-coupled monochromator (Zolix SBP 300) with 1 nm spectral resolution. The visible light spectra were detected using a photomultiplier tube with a 500 nm short cut filter. The near-infrared light spectra were detected using an InGaAs detector with a 800 nm short cut filter.

C. Time-resolved spectroscopy

To obtain the time-resolved spectra, a setup was built as shown in Fig. 2. P1 and P2 are Glan-Taylor polarizing prisms. The polarization directions of the excitation source and P1 are identical. The angle between this polarization direction and the optical axis of the electro-optic crystal in the electro-optic modulator is 45°. The electro-optic modulator was controlled by the output voltage of a high voltage power source to change the polarization direction of the excitation source, and triggered by a signal generator to adjust the frequency shift of this polarization. The polarization direction of P2 is vertical with respect to P1 in order to realize extinction. The excitation source intensity can be modulated by the waveform of the signal generator.

In our experiments, the excitation source was modulated by a square-wave and the decay curves were measured in the falling edge of the square-wave. The time-resolved spectra decayed from the steady-state due to the interaction between ions. The decay curves were recorded using a Tektronix DPO (5054) digital oscilloscope. All experiments were carried out at room temperature.

III. THEORETICAL MODEL

On the basis of the cooperative energy transfer process shown in Fig. 1, we propose a theoretical method of using rate equations to describe the dynamics of the energy transfer process. Neglecting the energy transfer from Yb^{3+} to Tb^{3+}, the energy transfer from $^5D_4$ of Tb^{3+} to higher excited levels and other processes, the rate equations for the excited-state population may be written as follows:

$$\frac{dn_1}{dt} = \sigma_{01}\rho n_0 - n_1 A_1 - w n_1 n_{0'}^2, \tag{1}$$

$$\frac{dn_2}{dt} = 2w n_1 n_{0'}^2 - n_2 A_2, \tag{2}$$

where n_0,n_1,$n_{0'}$, and n_2 are the energy level populations of $^7F_6$ (Tb^{3+}), $^5D_4$ (Tb^{3+}), $^2F_{7/2}$ (Yb^{3+}), and $^2F_{5/2}$ (Yb^{3+}), respectively; σ is the absorption cross section from the ground state of Tb^{3+}; $\rho$is the pump constant; A_1 and A_2 are the radiation rates of $^5D_4$ (Tb^{3+}) and $^2F_{5/2}$ (Yb^{3+}) levels, respectively; w is the corresponding parameter of the cooperative energy transfer process. The steady-state solution of the rate equations can be obtained:

$$n_1(0) = \frac{\sigma_{01}\rho n_0}{A_1 + w n_{0'}^2}, \tag{3}$$

$$n_2(0) = \frac{2w n_{0'}^2 \sigma_{01}\rho n_0}{(A_1 + w n_{0'}^2)A_2}. \tag{4}$$

Here, $n_2 \propto \rho$, $n_1 \propto \rho$, and both slopes of luminescence intensity versus the excitation power curves are 1 for Tb^{3+} and Yb^{3+}. This result is consistent with the expected linear process of down conversion. According to Eqs. (1) and (2), we can derive the following decay process:

$$n_1(t) = n_1(0)e^{-(A_1 + w n_{0'}^2)t} = n_1(0)e^{-t/\tau_1}, \tag{5}$$

$$n_2(t) = 2w n_{0'}^2 n_1(0)e^{-t/\tau_1} + n_2(0)e^{-t/\tau_2}. \tag{6}$$

Equation (5) contains the radiative decay term and the energy transfer term, which is similar to the decay signal expression of the donor ion in Eq. (11) of Ref. 9. From the expression of decay signal $n_2(t)$, the decay time contains two parts: $t_1 = \tau_1$ is the lifetime of Tb^{3+} energy level, and $t_2 = \tau_2$is the lifetime of Yb^{3+} energy level.

From the steady-state and dynamic solutions, we can derive two judgment criteria to test the cooperative quantum

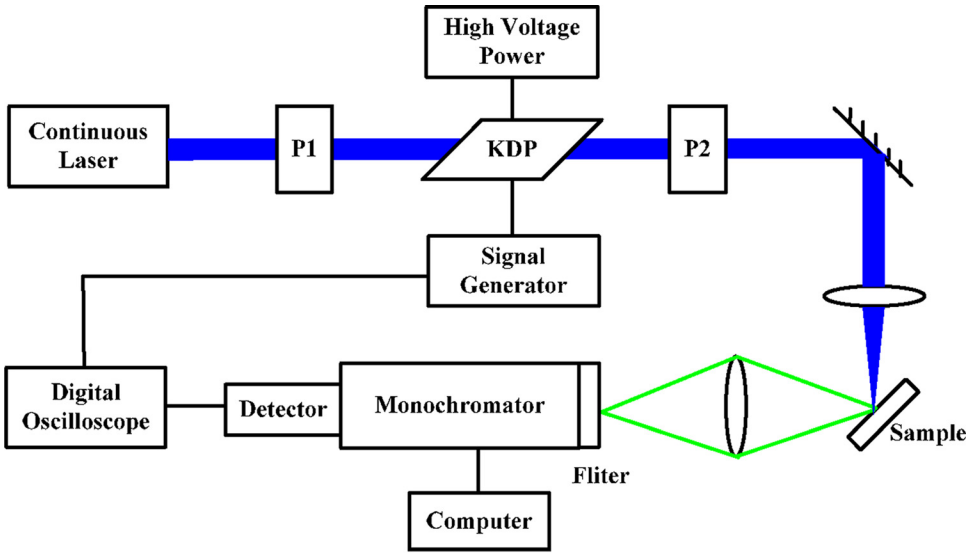

FIG. 2. (Color online) Time-resolved luminescence spectra measurement system (P1 and P2 are Glan-Taylor prisms).

cutting mechanism described by our rate equation model. One is the linear excitation power dependence, and the other is the correlation between the lifetimes of emissions from Tb^{3+} and Yb^{3+}.

IV. RESULTS AND DISCUSSION

Figure 3 depicts the emission spectra of $1Tb^{3+}$ doped and $1Tb^{3+}$-$5Yb^{3+}$ co-doped glass under the excitation of Tb^{3+} $^7F_6 \rightarrow {}^5D_4$ transition triggered by a 473 nm continuous wave laser. As shown in Figure 3, the emission bands centered at 542 nm, 585 nm, and 622 nm in the visible range are assigned to the transitions $^5D_4 \rightarrow {}^7F_J$ (J = 5,4,3), respectively. To verify these assignments we measured the decay curves and the power dependence of 542 nm, 585 nm, and 622 nm emissions. Both exhibit identical characteristics for these three emissions, which support our assignments.

The emission intensity of Tb^{3+} decreased with the introduction of Yb^{3+} and a broad near-infrared emission band around 1 μm appeared under the excitation of 473 nm laser. Because direct excitation at 473 nm is far from the resonant excitation for Yb^{3+}, this fact can be a proof of energy transfer from Tb^{3+} to Yb^{3+}. The near-infrared emission band includes two peaks: 982 nm and 1020 nm, which can be attributed to the stark splitting structure of Yb^{3+} $^2F_{5/2} \rightarrow {}^2F_{7/2}$ transition. Considering the energy level match relationship between Tb^{3+} and Yb^{3+}, the cooperative down conversion quantum cutting process from one Tb^{3+} to two Yb^{3+} is reasonable, as illustrated in Fig. 1.

To test the theoretical cooperative quantum cutting mechanism described by the rate equation model, the power dependence curves and time-resolved spectra of Tb^{3+} and Yb^{3+} were measured and are shown in Fig. 4. It can be seen that the intensities of Tb^{3+} and Yb^{3+} luminescence exhibit linear dependence on the excitation power. This indicates that the cooperative quantum cutting process in Tb^{3+}-Yb^{3+} co-doped glass is a linear process. The result is consistent with the first judgment criterion of our rate equation model.

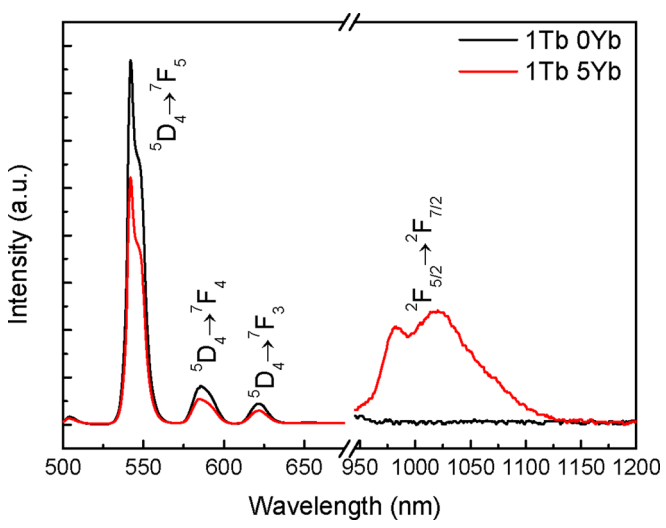

FIG. 3. (Color online) Emission spectra of $1Tb^{3+}$ single-doped and $1Tb^{3+}$-$5Yb^{3+}$ co-doped glass under a 473 nm continuous wave laser excitation.

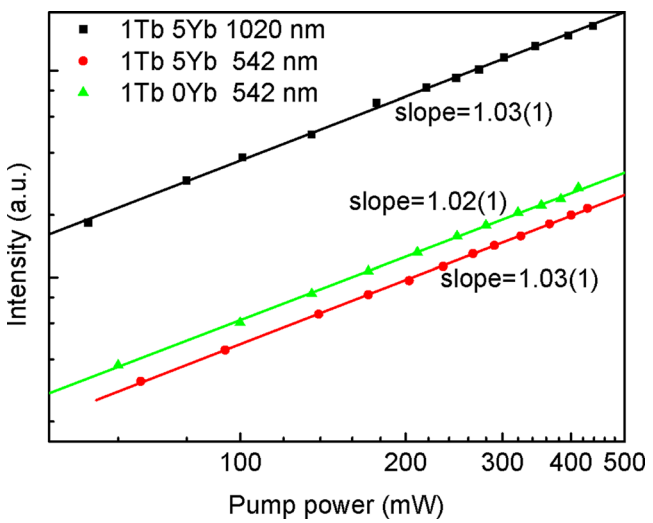

FIG. 4. (Color online) Double logarithmic plot of Tb^{3+} and Yb^{3+} emission intensities vs the pump power of 473 nm laser for $1Tb^{3+}$ single-doped and $1Tb^{3+}$-$5Yb^{3+}$ co-doped glass.

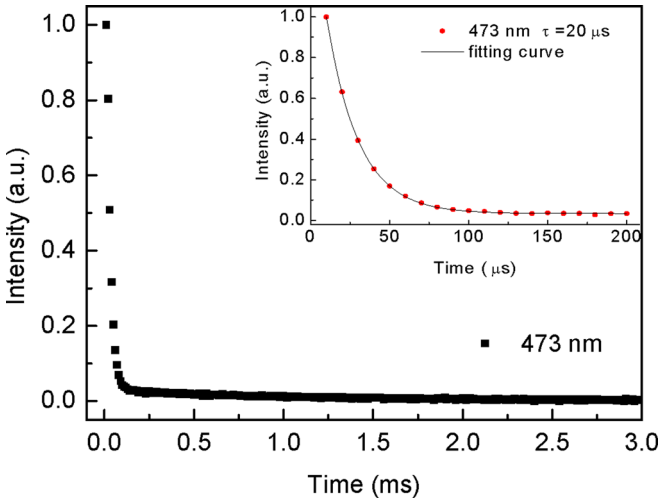

FIG. 5. (Color online) The response time of measurement system at 473 nm. The inset shows an amplification of partial decay curve of the measurement system at 473 nm.

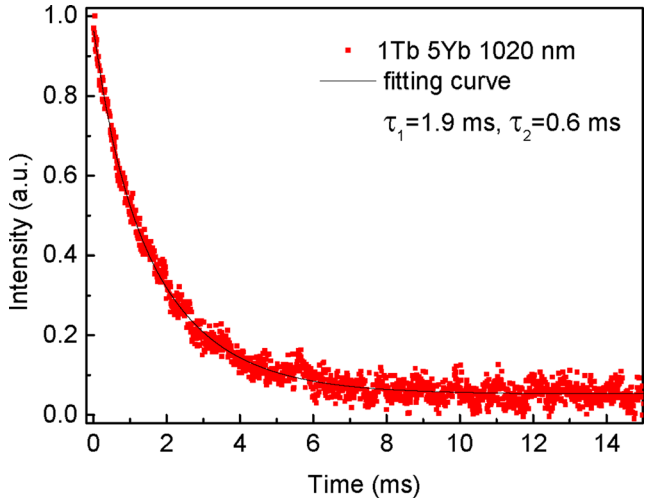

FIG. 7. (Color online) Luminescence decay curves of Yb^{3+} $^2F_{5/2}\rightarrow{}^2F_{7/2}$ transition at 1020 nm in $1Tb^{3+}$-$5Yb^{3+}$ co-doped glass under 473 nm excitation.

The system response time was measured and shown in Fig. 5. The inset is an amplification of the partial decay curve of the measurement system at 473 nm. Fitting the decay curve with an exponential function gives the system response time of about 20 μs, which can be neglected in the measurement of lifetimes (in the order of ms).

The luminescence decay curves of Tb^{3+} 542 nm emission, originated from the $^5D_4\rightarrow{}^7F_5$ transition, are plotted in Fig. 6. Fitting the decay curves to an exponential function provided the decay times of 2.5 ms and 2.0 ms for Tb^{3+} doped and $1Tb^{3+}$-$5Yb^{3+}$ co-doped glass, respectively. A typical decay time for Tb^{3+} $^5D_4$ level is between 2 and 3 ms according to the literature.[9,10,12,23] The measurement results showed that our measurement system is reliable. The decay time of Tb^{3+} decreased noticeably when 5% Yb^{3+} is introduced, which can be attributed to an extra decay pathway provided by Yb^{3+}. This can serve as another evidence of the energy transfer from Tb^{3+} to Yb^{3+}.

Figure 7 shows the luminescence decay curve of Yb^{3+} 1020 nm emission originated from the $^2F_{5/2}\rightarrow{}^2F_{7/2}$ transition in $1Tb^{3+}$-$5Yb^{3+}$ co-doped glass. Fitting the decay curves with a double-exponential function, we found that the decay curve actually consists of two parts: a slow decay time of 1.9 ms and a fast decay time of 0.6 ms. A typical lifetime of Yb^{3+} $^2F_{5/2}$ level is hundreds of microseconds, according to previous reports.[9,23,24] To further determine the lifetime of the energy level of Yb^{3+}, we measured the luminescence decay curve of Yb^{3+} 1020 nm emission under a 980 nm diode laser excitation. The lifetimes of Yb^{3+} in $1Tb^{3+}$-$5Yb^{3+}$ and $5Yb^{3+}$ doped glass are 0.5 ms and 0.6 ms, respectively (shown in Fig. 8). Therefore, we believe that the 0.6 ms is the lifetime of the Yb^{3+} $^2F_{5/2}$ energy level. The slow decay time of 1.9 ms is close to the lifetime of the Tb^{3+} $^5D_4$ energy level (2 ms). The correlation between 1.9 ms and 0.6 ms is in good agreement with the dynamic solution of our rate equation model (Eq. (6)). A similar phenomenon has been observed in $1Tb^{3+}$-$10Yb^{3+}$ co-doped glass. This result supports the second judgment criterion of our rate equation model, therefore, it can serve as a direct proof for the energy

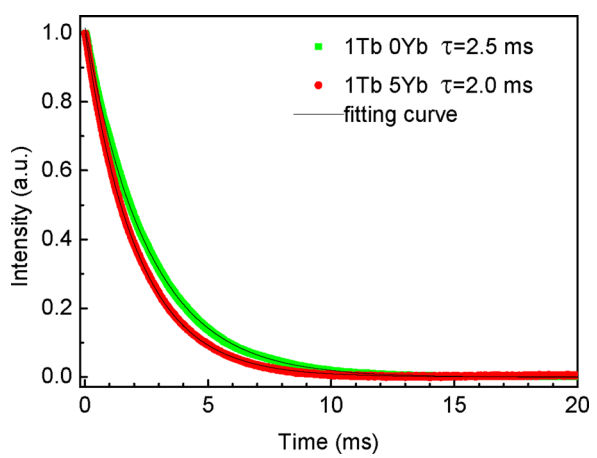

FIG. 6. (Color online) Luminescence decay curves of Tb^{3+} $^7F_6\rightarrow{}^5D_4$ transition at 542 nm in $1Tb^{3+}$ single-doped and $1Tb^{3+}$-$5Yb^{3+}$ co-doped glass under 473 nm excitation.

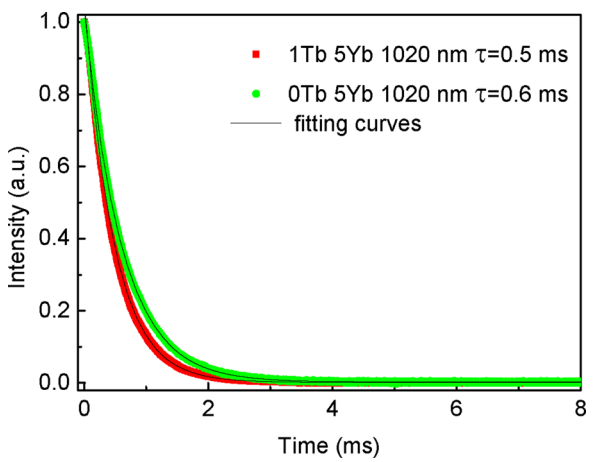

FIG. 8. (Color online) Luminescence decay curves of Yb^{3+} $^2F_{5/2}\rightarrow{}^2F_{7/2}$ transition at 1020 nm in $1Tb^{3+}$-$5Yb^{3+}$ and $0Tb^{3+}$-$5Yb^{3+}$ co-doped glass under 980 nm excitation.

transfer from Tb^{3+} to Yb^{3+}. It also further confirmed the cooperative quantum cutting mechanism in Tb^{3+}-Yb^{3+} co-doped oxyfluoride glass.

Using the parameters of rate equations, the overall quantum efficiency η of cooperative down conversion in Tb^{3+}-Yb^{3+} is defined as the ratio of emission photon number to the absorbed photon number, while the near-infrared quantum efficiency η_{NIR} is the ratio of Yb^{3+} emission photon number to the absorbed photon number. The corresponding equations are:

$$\eta = \frac{n_1 A_1 + n_2 A_2}{n_0 \rho \sigma_{01}} = \frac{A_1 + 2wn_{0'}^2}{A_1 + wn_{0'}^2} = 1 + \left(1 - \frac{\tau}{\tau_0}\right), \quad (7)$$

$$\eta_{NIR} = \frac{n_2 A_2}{n_0 \rho \sigma_{01}} = \frac{2wn_{0'}^2}{A_1 + wn_{0'}^2} = 2\left(1 - \frac{\tau}{\tau_0}\right), \quad (8)$$

$$\tau_0 = \frac{1}{A_1}, \quad \tau = \frac{1}{A_1 + wn_{0'}^2}, \quad (9)$$

where τ and τ_0 are the lifetimes of Tb^{3+} $^5D_4$ energy level with and without Yb^{3+} doping, respectively. This quantum efficiency equation is consistent with previously reported definitions, which were defined based on the energy transfer efficiency.[9] The correct prediction of the quantum efficiency is another proof that our rate equation model is sound and fairly powerful. On the basis of the definitions given in Eqs. (7) and (8), the overall quantum efficiency and the near infrared quantum efficiency in $1Tb^{3+}$-$5Yb^{3+}$ co-doped glass are 120% and 40%, respectively.

It should be noted that the cooperative quantum cutting process is not always linear. We found that the fitted slopes of Yb^{3+} luminescence power dependence curves were $0.6 \sim 0.8$ in fluoride powder samples, for which the linear process coexists with the second-order process. Therefore, the slope of Yb^{3+} luminescence power dependence curve can reflect the physical nature in the quantum cutting process between Tb^{3+} and Yb^{3+} ions in different host materials.

V. CONCLUSIONS

In summary, the quantum cutting energy transfer mechanisms in Tb^{3+}-Yb^{3+} co-doped oxyfluoride glass have been investigated both theoretically and experimentally. We propose a rate equation model to describe the quantum cutting process. Unlike earlier models, our model includes information of both donor ion Tb^{3+} and acceptor ion Yb^{3+}. Two judgment criteria were derived: (1) linear excitation power dependence; and (2) a correlation exists between the time-resolved luminescence spectra of donor and acceptor ions. An experimental system was designed and built to measure the time-resolved spectra under the excitation of a 473 nm continuous wave laser. From the emission spectra and the time-resolved spectra, one can conclude that the energy is indeed transferred from Tb^{3+} to Yb^{3+}, and the overall quantum efficiency is 120% when there is 5% Yb^{3+} doping. The down conversion emission intensities increase linearly with the excitation power. The overall lifetime of Yb^{3+} not only consists of its own lifetime but also the lifetime of donor ion Tb^{3+}, showing the inter-ionic interactions. Our experimental results meet the two judgment criteria of the rate equation model, which was proposed based on a cooperative energy transfer process. The agreement between the experimental results and the theoretical model further confirmed the cooperative quantum cutting mechanism in Tb^{3+}-Yb^{3+} co-doped oxyfluoride glass.

ACKNOWLEDGMENTS

This work was supported by the Natural Science Foundation of Heilongjiang Province, People's Republic of China under Grant No. A 200503 and the Key Scientific and Technology Project of Harbin City Bureau of Science and Technology under Grant No. 2009AA3BS131.

[1]W. Shockley and H. J. Queisser, J. Appl. Phys. **32**, 510 (1961).
[2]B. S. Richards, Sol. Energy Mater. Sol. Cell. **90**, 2329 (2006).
[3]T. Trupke, M. A. Green, and P. Wurfel, J. Appl. Phys. **92**, 1668 (2002).
[4]B. S. Richards, Sol. Energy Mater. Sol. Cell. **90**, 1189 (2006).
[5]R. T. Wegh, H. Donker, K. D. Oskam, and A. Meijerink, Science. **283**, 663 (1999).
[6]G. H. Dieke and H. M. Crosswhite, Appl. Opt. **2**, 675 (1963).
[7]R. T. Wegh, A. Meijerink, R.- J. Lamminmäki, and H. Jorma, J. Lumin. **87-89**, 1002 (2000).
[8]Q. Y. Zhang and X. Y. Huang, Prog. Mater. Sci. **55**, 353 (2010).
[9]P. Vergeer, T. J. H. Vlugt, M. H. F. Kox, M. I. den Hertog, J. P. J. M. van der Eerden, and A. Meijerink, Phys. Rev. B. **71**, 014119 (2005).
[10]Q. Y. Zhang and G. F. Yang, Appl. Phys. Lett. **91**, 051903 (2007).
[11]J. L. Yuan, X. Y. Zeng, J. T. Zhao, Z. J. Zhang, H. H. Chen, and X. X. Yang, J. Phys D. **41**, 105406 (2008).
[12]S. Ye, B. Zhu, J. X. Chen, J. Luo, and J. R. Qiu, Appl. Phys. Lett. **92**, 141112 (2008).
[13]X. P. Chen, X. Y. Huang, and Q. Y. Zhang, J. Appl. Phys. **106**, 063518 (2008).
[14]B. M. van der Ende, L. Aarts, and A. Meijerink, Adv. Mater. **21**, 3073 (2009).
[15]S. Ye, B. Zhu, J. Luo, J. X. Chen, G. Lakshminarayana, and J. R. Qiu, Opt. Exp. **16**, 8989 (2008).
[16]M. Pollnau, D. R. Gamelin, S. R. Lüthi, and H. U. Güdel, Phys. Rev. B. **61**, 3337 (2000).
[17]D. L. Dexter, Phys. Rev. **108**(3), 630 (1957).
[18]B. M. van der Ende, L. Aarts, and A. Meijerink, Phys. Chem. Chem. Phys. **11**, 11081 (2009).
[19]W. Strek, A. Bednarkiewicz, P. J. Dereń, J. Lumin. **92**, 229 (2001).
[20]D. Q. Chen, Y. L. Yu, Y. S. Wang, P. Huang, and F. Y. Weng, J. Phys. Chem. C. **113**, 6406 (2009).
[21]D. Q. Chen, Y. S. Wang, Y. L. Yu, P. Huang, and F. Y. Weng, J. Appl. Phys. **104**, 116105 (2008).
[22]Y. Teng, J. J. Zhou, X. F. Liu, S. Ye, and J. R. Qiu, Opt. Exp. **18**, 9671 (2010).
[23]Q. Zhang, X. F. Liu, S. Ye, B. Zhu, Y. B. Qiao, G. P. Dong, B. Qian, D. P. Chen, Q. L. Zhou, and J. R. Qiu, IEEE Photon. Technol. Lett. **21**, 1169 (2009).
[24]L. Aarts, B. M. van der Ende, M. F. Reid, and A. Meijerink, Spectrosc. Lett. **43**, 373 (2010).